










Fast and Miniaturized Phase Shifter With Excellent Figure of Merit Based on Liquid Crystal and Nanowire-Filled Membrane Technologies

DONGWEI WANG ¹, ERSIN POLAT ¹ (Student Member, IEEE),
CHRISTIAN SCHUSTER ¹ (Student Member, IEEE), HENNING TESMER ¹ (Student Member, IEEE),
GUSTAVO P. REHDER ² (Member, IEEE), ARIANA L. C. SERRANO ² (Member, IEEE),
LEONARDO G. GOMES ² (Graduate Student Member, IEEE), PHILIPPE FERRARI ³ (Senior Member, IEEE),
HOLGER MAUNE ⁴ (Senior Member, IEEE), AND ROLF JAKOBY¹ (Member, IEEE)

(Regular Paper)

¹Institute of Microwave Engineering and Photonics (IMP), Technische Universität Darmstadt, 64289 Darmstadt, Germany

²LME, Escola Politécnica da Universidade de São Paulo, São Paulo 05508-010, Brazil

³RFIC-Lab, Grenoble INP, Université Grenoble Alpes, 38000 Grenoble, France

⁴Microwave and Communication Engineering Department, University of Magdeburg, 39106 Magdeburg, Germany

CORRESPONDING AUTHOR: Dongwei Wang (e-mail: dongwei.wang@tu-darmstadt.de).

This work was supported by Deutsche Forschungsgemeinschaft (DFG) and the Brazilian agency CNPq within projects JA921/65-1 and 431200/18-1, respectively, and the Open Access Publishing Fund of the Technical University of Darmstadt.

ABSTRACT This paper presents a highly miniaturized tuneable microstrip line phase shifter for 5 GHz to 67 GHz. The design takes advantage of the microstrip topology by substituting the ground plane by a metallic-nanowire-filled porous alumina membrane (NaM). This leads to a slow-wave (SW) effect of the transmission line; thus, the transmission line can be physically compact while maintaining its electric length. By applying a liquid crystal (LC) with its anisotropic permittivity as substrate between the transmission line and the NaM, a tuneable microstrip line phase shifter is realized. Three demonstrators are identically fabricated filled with different types of high-performance microwave LCs from three generations (GT3-23001, GT5-26001 and GT7-29001). The measurement results show good matching in a 50 Ω system with reflection less than -10 dB over a wide frequency range. These demonstrators are able to reach a maximum figure of merit (FoM) of 41 $^{\circ}$ /dB, 48 $^{\circ}$ /dB, and 70 $^{\circ}$ /dB for different LCs (GT3-23001, GT5-26001 and GT7-29001, respectively). In addition, experiments show that all three LCs should be biased with square wave voltage at approximately 1 kHz to achieve maximum tuneability and response speed. The achieved response times with GT3-23001, GT5-26001 and GT7-29001 are 116 ms, 613 ms, and 125 ms, respectively, which are much faster than other reported LC phase shifter implementations. Large-signal analysis shows that these implementations have high linearity with third-order interception (IP3) points of approximately 60 dBm and a power handling capability of 25 dBm.

INDEX TERMS IP3, liquid crystal, microstrip line, nanowires, phase shifter, slow-wave, S-parameter.

I. INTRODUCTION

As demand for higher data rates in wireless communication systems is increasing rapidly, 20, 40 and even 100 Gbps rates are expected for wireless technologies. To achieve such

high data rates, large absolute bandwidths are required, which are available at millimeter-waves (mmW) frequencies. To overcome the high free space loss, antenna arrays are proposed with high gain and corresponding narrow beams. Beam

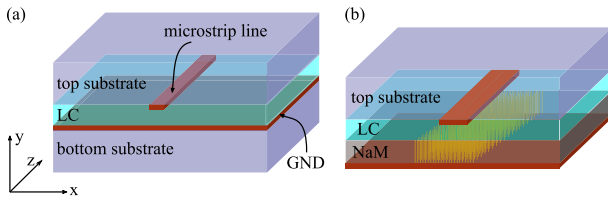


FIGURE 1. Schematic of (a) Conventional LC based microstrip line (LC-MS) phase shifter and (b) proposed LC-NaM phase shifter.

steering of the array enables the steering of its main beam to the desired angle to maximize the communication quality. For electric passive beam steering, phase shifters are key components and are desired to have high reliability, high performance and fast response time at low cost.

There are several technologies available to realize phase shifters. Those based on RF microelectromechanical systems (RF MEMS) have been demonstrated in [1]–[3]. They offer high performance in terms of maximum phase shift, insertion loss (IL), and power consumption. However, RF MEMS are comparatively fragile against wear out failures, and are difficult to integrate into antenna arrays due to phase errors induced by their discrete phase change. Phase shifters using barium strontium titanate (BST) are presented in [4]–[6]. BST-based devices provide sufficiently high performance only up to the X-band and degrade considerably beyond this frequency range [7]. In addition to BST, liquid crystals (LCs) represent another promising tuneable dielectric, but generally above 5 GHz, even up to at least 8 THz [8]–[10]. These materials provide continuous tuneability, high linearity and low loss at low cost by using standard technologies. Applications implementing LCs in tuneable devices have been proposed, such as tuneable filters [11], [12], phase shifters [13]–[15], and based on them, steerable phased arrays [13], [16].

The three generations of LC mixtures used in this paper are in the nematic phase, in which the LC is considered a uniaxial anisotropic material because of its rod-like molecules [17], [18]. When electromagnetic waves pass through the LC, it exhibits different permittivities, depending on the orientation of the LC molecules to the RF field.

Fig. 1(a) demonstrates the conventional way to use an LC as a tuneable dielectric in a microstrip topology to realize a phase shifter (LC-MS), where a “substrate-microstrip line-LC-ground-substrate” structure is widely utilized. The proposed phase shifter substitutes the ground and bottom substrate with NaM (LC-NaM), as shown in Fig. 1(b). They have the same working principle: In the unbiased state as in Fig. 2(a), due to surface anchoring, nearly all LC molecules are perpendicular to the RF field. Hence, the RF field experiences a relative permittivity of $\epsilon_{r,\perp}$ and loss tangent $\tan \delta_{\perp}$. When a bias AC voltage V_B is applied between the signal electrode and the ground electrode, as shown in Fig. 2(b), the LC molecules orient towards the biasing E-field lines until they are in parallel to the biasing field. Hence, the RF field experiences a material’s relative permittivity, which varies from $\epsilon_{r,\perp}$ continuously towards $\epsilon_{r,\parallel}$, accompanied by a change

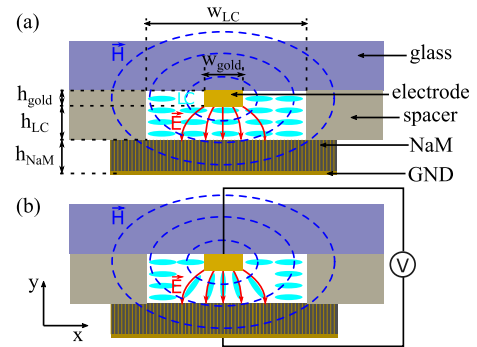


FIGURE 2. Cross section of the LC-NaM phase shifter from Fig. 1(b) and its working principle. (a) Unbiased, LC molecules are parallel to the xz-plane and perpendicular to the RF E field. (b) Fully biased, parallel orientation. $h_{\text{gold}} = 2 \mu\text{m}$, $h_{\text{LC}} = 4 \mu\text{m}$, $w_{\text{LC}} = 500 \mu\text{m}$, $w_{\text{gold}} = 25 \mu\text{m}$, $h_{\text{NaM}} = 50 \mu\text{m}$.

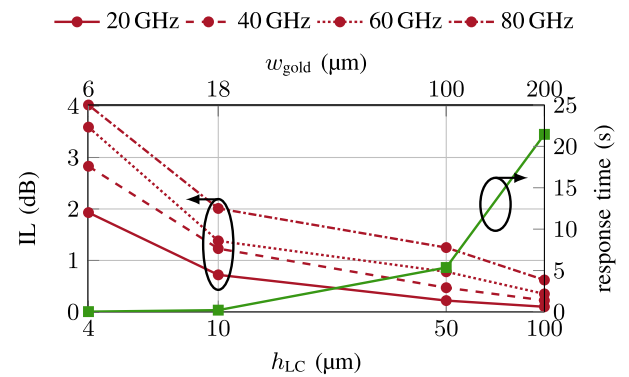


FIGURE 3. Simulated IL and response time of the LC-MS phase shifter shown in Fig. 1(a) with respect to h_{LC} at different frequencies. AF32 glass is used as a substrate in the simulation with a fixed thickness of $700 \mu\text{m}$, relative dielectric constant $\epsilon_r = 5.1$ and loss tangent $\tan \delta = 0.01$. The LC parameters are given below. The response time is independent of RF frequency. Z_c is kept at 50Ω during simulation by using the proper line width w_{gold} corresponding to h_{LC} .

in the loss tangent from $\tan \delta_{\perp}$ to $\tan \delta_{\parallel}$. Once the bias is released, the LC molecules recover their initial orientation by the anchoring force.

LC-MS have been reported in [16], [19]–[21], from which several conclusions can be drawn:

- 1) The IL is dominated by the conductor loss of the strip electrode, especially for increasing frequency.
- 2) To reduce the IL, an increased microstrip line width is required. Moreover, the LC layer thickness increases proportionally to maintain a constant characteristic impedance Z_c of the microstrip line, normally 50Ω .
- 3) However, a thicker LC layer leads to a longer response time of LC molecules, which will be discussed in Section III.

In other words, reducing the response time and lowering the IL have mutually contrary requirements with respect to LC thickness. A comparison of the IL and response time with varied LC layer thickness h_{LC} is performed by using CST Microwave Studio (CST) simulation as shown in Fig. 3. Similar comparison results are also available in [19], [20].

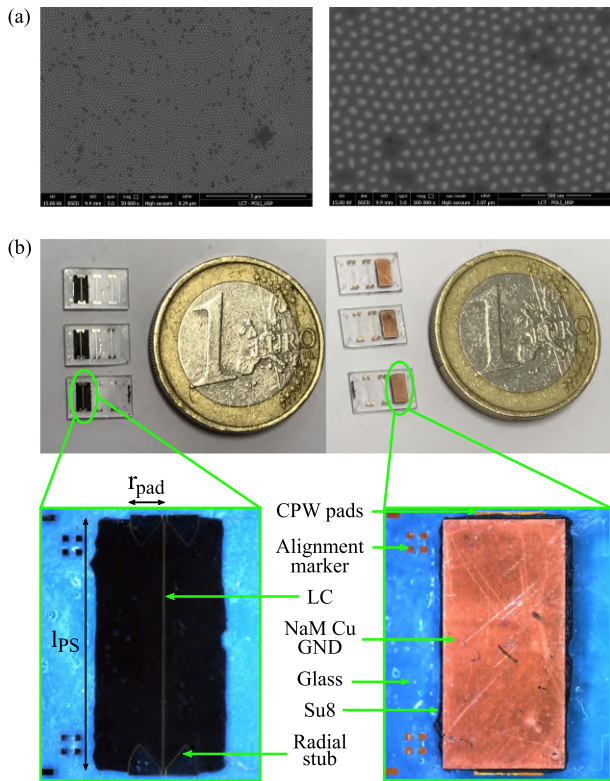


FIGURE 4. (a) Top side of the NaM sample under an electron microscope. (b) Top and bottom sides of tuneable LC-NaM phase shifter as in Fig. 1(b). The dimensions are given as follows: radial pad radius $r_{\text{pad}} = 470 \mu\text{m}$ and phase shifter line length $l_{\text{PS}} = 3600 \mu\text{m}$.

To solve this issue, considerable efforts have been invested to combine LCs with high-performance slow-wave (SW) transmission lines (TLs). Planar SW TLs have been successfully demonstrated in microstrip [22], [23] and coplanar waveguide topology [24], [25], where TLs are periodically loaded with lumped reactances. However, these technologies suffer from high complexity, sometimes high cost, limited bandwidth and relatively high IL. Recently, SW TLs based on NaM have provided a novel approach, with high performance, low cost and easy fabrication [26]–[28]. NaM is fabricated based on a commercial porous alumina membrane. These nanopores are periodically and regularly distributed with a pore diameter and an interpore pitch of approximately 50 nm and 150 nm, respectively. Copper is first sputtered on the bottom side of the membrane, and then, copper nanowires are grown into these nanopores by electrodeposition until they reach the top side. Finally, the top side is polished down to the desired thickness to ensure that the nanowires are isolated from each other on the top side, as shown in Fig. 4(a). The NaM fabrication procedure is described in detail in [26]–[28]. By implementing NaM in microstrip topology, the electric field of the RF signal is mostly captured by the nanowires on the top surface of the NaM and barely penetrates into it. In contrast, the magnetic field is almost unperturbed due to the extremely thin diameter of the nanowires [28], compare Fig. 2. This design results in

a significant increase in the distributed capacitance (C') and distributed inductance (L') of the TL. According to

$$v_{\phi} = \sqrt{\frac{1}{L' \cdot C'}} = f \cdot \lambda \quad \text{and} \quad Z_c = \sqrt{\frac{L'}{C'}} \quad (1)$$

the phase velocity v_{ϕ} decreases, and the wavelength λ , while Z_c can remain 50Ω . Previous research on LC-NaM [29] preliminarily demonstrates this principle. However, due to non-optimal design and fabrication, its performance is rather poor compared to state-of-the-art LC phase shifters, e.g. long response time, high IL, low phase shift. It used laser cutting to get NaM of desired dimensions, since NaM is easily broken by saw dicing. However, later investigation shows that NaM melts during laser cutting and the coagulum forms edge with several μm thickness. This results in much higher h_{LC} which deteriorates the impedance matching and response. Besides, the copper ground of NaM is partially delaminated from the alumina membrane caused by the high temperature, where the electric potential of the nanowires is undefined. This deteriorates the LC tuning efficiency and SW effect. In this work, NaM is etched by sodium hydroxide (NaOH) solution with the help of a mask. Although with relatively rough edges as in Fig. 4(b), the aforementioned issues are solved. In addition, specifically scratched polymer layers for LC alignment are processed on both NaM and substrate for improving the tuning speed and FoM.

In this paper, an improved version of LC-NaM is proposed which outperforms the previous version in [29]. In Section II, the simulation and measurement results of three demonstrator batches are presented: first without LC (air filled) and then filled with three generations of advanced microwave LCs. The influence of bias on LC tuneability is studied in Section III. Large-signal measurement is investigated in Section IV, and finally, a conclusion is given in Section V.

II. SLOW-WAVE PHASE SHIFTER

According to Fig. 1(b), an LC-NaM phase shifter is fabricated and shown in Fig. 4(b). The electrode and spacers located on the top side of glass substrate are processed by a standard lithography process: chromium (Cr) / gold (Au) seed layer evaporation, photolithography, Au electroplating, wet etching, spacer patterning, polymer layer coating and scratching. Then, etched NaM pieces are flip-chipped onto the substrate and precisely aligned under a microscope. Next, ultraviolet (UV) curable glue is applied to fix the structure. AF32 glass from Schott AG is good for both alignment and UV curing of the glue because of its transparency. In addition, this glass provides good mechanical stability and electric properties. Afterwards, the LC is filled into the cavity by means of capillary forces. Finally, the samples are kept in a vacuum chamber to eventually remove air bubbles. During this time, due to unbalanced air pressure inside and outside the bubbles, encapsulated air inside the bubble will press itself into vacuum. The LC itself is well sealed inside the cavity by surface tension. The microstrip line width w_{gold} and thickness h_{gold} are well controlled to be $25 \mu\text{m}$ and $2 \mu\text{m}$, respectively. The thickness

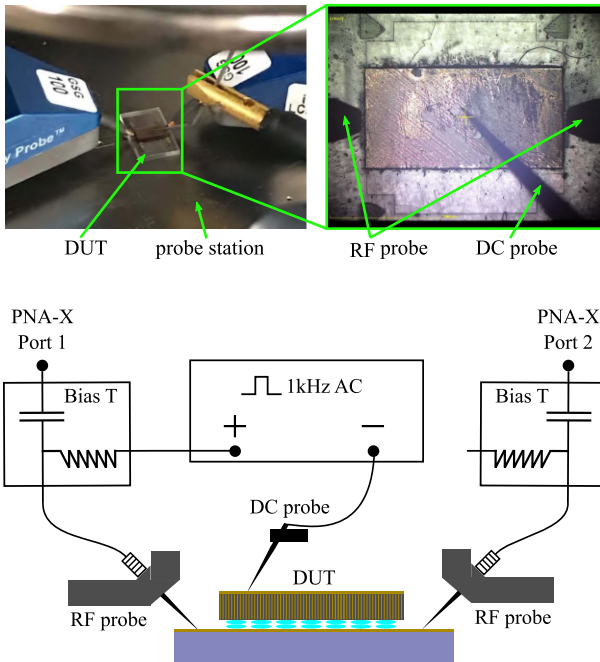


FIGURE 5. Measurement setup for the S-parameters. Phase shifters are the device under test (DUT).

of spacers is $6 \mu\text{m}$, leading to $h_{\text{LC}} = 4 \mu\text{m}$. These dimensions provide a microstrip line Z_c of 50Ω when filled with LCs.

A. SLOW-WAVE TRANSMISSION LINE WITHOUT LCs

The first measurement is carried out on three identical batches before LCs are filled in to examine the workability and feasibility of the fabrication process under a simplified situation and to serve as reference. The three demonstrators are characterized by means of on-wafer measurements, using PNA-X from Keysight Technologies and I67-GSG-100 probes from Formfactor, from 100 MHz to 67 GHz, with line-reflect-reflect-match (LRRM) probe tip calibration. The measurement setup is shown in Fig. 5. The measured scattering S-parameters of the three identical demonstrators with air filling, as well as the simulated results according to full-wave simulations using CST, are given in Fig. 6. The NaM parameters used in simulation is $(\epsilon_{r,x}, \epsilon_{r,y}, \epsilon_{r,z}) = (6.7, 20000, 6.7)$ and conductivity $(\sigma_x, \sigma_y, \sigma_z) = (0, 5.96e7, 0)$ to represent its metallic and dielectric behaviors in y and x,z directions, respectively. The demonstrators show good agreement with each other and with simulation from 0 GHz to 67 GHz in terms of transmission coefficient $|S_{21}|$ and reflection coefficient $|S_{11}|$, which indicates a decent repeatability of the fabrication and validity of simulation model. In particular, the cavity heights of the demonstrators can be considered identical, which is the premise for the following comparison between LCs. From Fig. 6, $|S_{11}|$ have strong resonance behaviour. The reason is that the transmission lines are designed to work with LCs ($\epsilon_r \approx 2.4$ to 3.5), which leads to a distinct impedance mismatch when filled with air ($\epsilon_r = 1$).

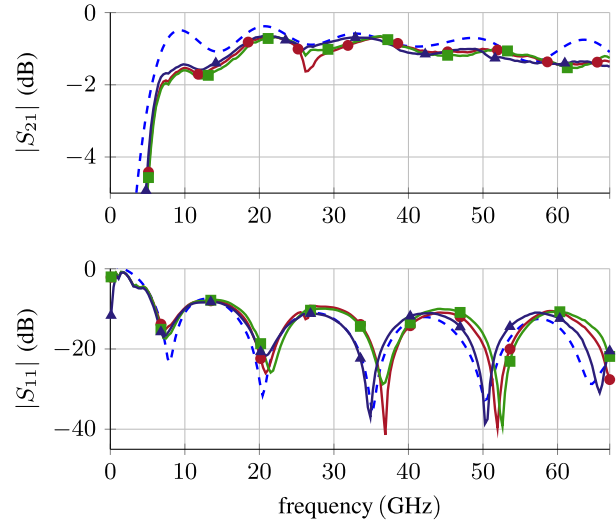


FIGURE 6. Measured and simulated results of three identical demonstrators filled with air.

TABLE 1. LC Properties Used in Simulation and Calculation [10], [17], [30]

LC Type	$\epsilon_{r,\parallel}$	$\tan \delta_{\parallel}$	$\epsilon_{r,\perp}$	$\tan \delta_{\perp}$
GT3-23001	3.28	0.0038	2.46	0.0143
GT5-26001	3.27	0.0022	2.39	0.007
GT7-29001	3.53	0.0064	2.45	0.0116

B. SLOW-WAVE PHASE SHIFTER WITH LC

The three demonstrators are then filled with three generations of LC mixtures, namely, GT3-23001, GT5-26001 and GT7-29001, respectively, from Merck KGaA, Darmstadt, Germany. The properties of the three types of LCs are listed in Table 1. During the measurement, DC (0 Hz) and square wave voltages from 10 Hz to 10 kHz are applied between the electrode and NaM in the range of 0 V to 20 V in steps of 1 V. The electric characteristics of the tuneable phase shifters remain nearly constant for bias voltages higher than 10 V. An important parameter used for quantifying the RF performance of a phase shifter is the frequency-related FoM, which is defined by the ratio of the maximum phase shift over the highest IL among the two extreme LC alignment cases [17]:

$$\text{FoM} = \frac{\Delta\phi_{b,\text{max}}}{\text{IL}_{\text{max}}} \quad (2)$$

Fig. 7 presents the measured and simulated S-parameters in both unbiased ($V_B = 0 \text{ V}$) and fully biased cases ($V_B = 10 \text{ V}$). Phase shift $\Delta\phi_{b,\text{max}}$ is the phase difference of S_{21} between the two bias cases. The measured and simulated $\Delta\phi_{b,\text{max}}$ and FoMs are plotted in Fig. 8. Above 5 GHz, all three demonstrators match 50Ω with $|S_{11}| \leq -10 \text{ dB}$ in both bias cases. The GT3 demonstrator has a FoM higher than $30^\circ/\text{dB}$ above 25 GHz and higher than $40^\circ/\text{dB}$ between 52 GHz and 65 GHz, while the maximum value is $41^\circ/\text{dB}$ at 52 GHz. The FoM of the GT5 demonstrator remains higher than $30^\circ/\text{dB}$ above

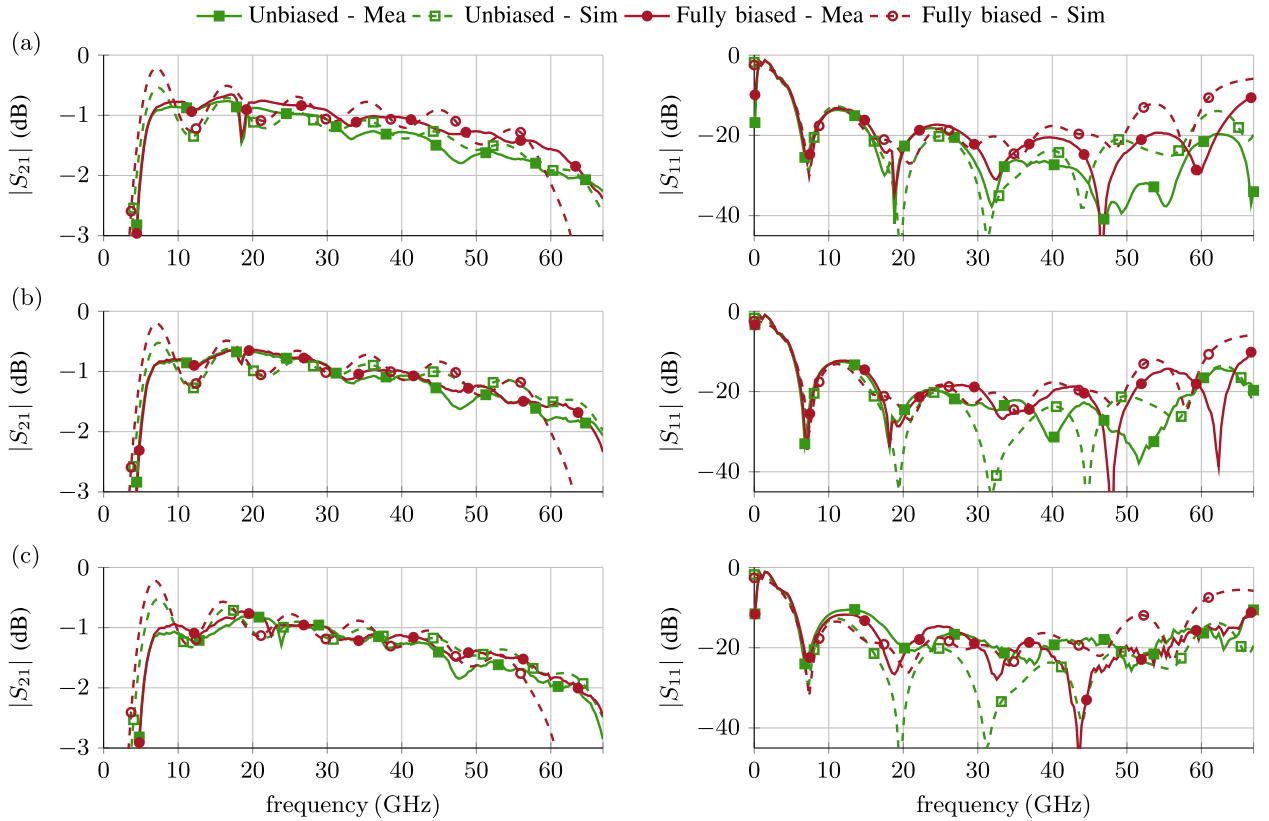


FIGURE 7. Measured and simulated results of demonstrators filled with (a) GT3-23001, (b) GT5-26001, and (c) GT7-29001.

17 GHz and maximizes at 52 GHz with 48 °/dB. The behaviour of the GT7 demonstrator improves by a large margin; its FoM remains higher than 30 °/dB above 15 GHz and higher than 50 °/dB above 25 GHz. The maximum FoM is 70 °/dB at 43 and 56 GHz. As seen from Fig. 7, the IL in the fully biased case is generally less than that in the unbiased case because the LC is more lossy with perpendicular polarization than with parallel polarization; see Table 1. According to Fig. 8, for the GT3 and GT5 demonstrators, the differences between the measured and simulated results are quite obvious, while GT7 shows less difference. The reason is that the inner surfaces of LC cavities provide insufficient and different anchoring forces to different LCs, and that the microstrip topology has fringing fields. The LC parameters given in Table 1 cannot be utilized completely in practical devices.

In Fig. 4, coplanar waveguide (CPW) pads at both line ends are designed for on-wafer measurement. Instead of using vias, radial stubs have been used for simplification of the production process. The radial stubs perform as an open-ended $\lambda/4$ -transformer to couple the grounds of the CPW to NaM, which is the ground of the microstrip line [31], [32]. This approach provides a smooth and broadband CPW to microstrip mode transition from approximately 5 GHz to 60 GHz, beyond which the parasitics of the via-less transitions are significant.

TABLE 2. Measured τ_{on} and τ_{off} of Three Demonstrators With $h_{\text{LC}} = 4 \mu\text{m}$ at 1 kHz

	GT3-23001	GT5-26001	GT7-29001
τ_{on} (ms)	9.4	106	3.1
τ_{off} (ms)	116	613	125

III. LC TUNING VERSUS BIAS FREQUENCY

The response time of LC phase shifter is characterized by the switch-on (τ_{on}) and the switch-off (τ_{off}) response time. They define the time for rising from 10% to 90% of $\Delta\phi_{\text{b,max}}$ after bias is applied, and falling from 90% to 10% once bias vanishes. Phase of S_{21} ($\angle S_{21}$) at 60 GHz is measured. Fig. 9 describes the response times of the demonstrators tuned by 1 kHz square wave of 10 V. τ_{on} and τ_{off} for all three demonstrators are measured and listed in Table 2. GT3 and GT7 achieve 100 ms level response time, while GT5 has 613 ms due to its higher viscosity.

The influence of the bias frequency on τ_{off} is given in Fig. 10(a), from which it is concluded that the LC biased by DC voltage generally takes a longer time to realign.

Fig. 10(b) shows the differential phase shift $\Delta\phi_{\text{b,max}}$ versus the AC bias frequency. The phase shifts for all three

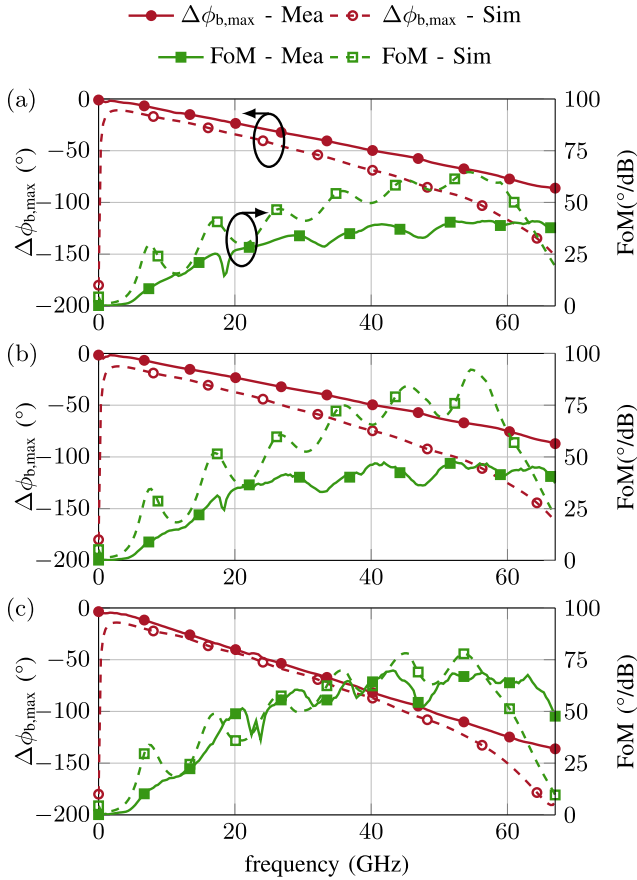


FIGURE 8. Measured and simulated FoM and $\Delta\phi_{b,max}$ of demonstrators filled with (a) GT3, (b) GT5, and (c) GT7.

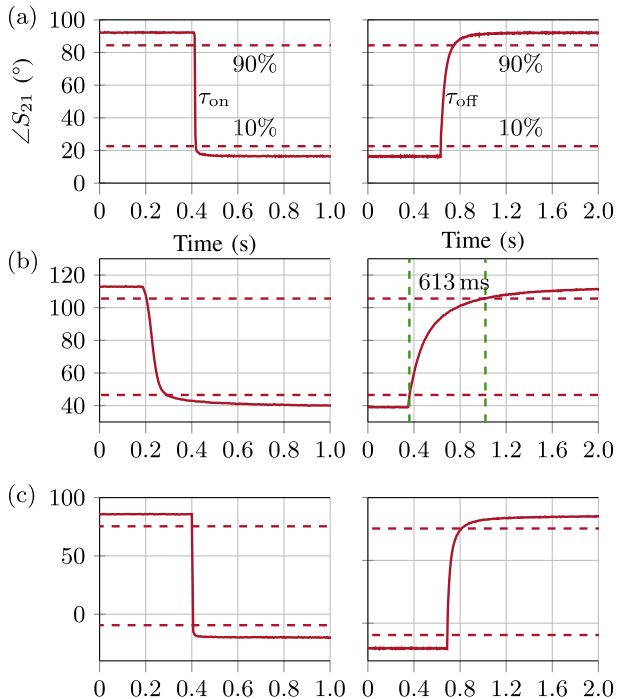


FIGURE 9. Measurement results of the response time τ_{on} and τ_{off} of demonstrators filled with (a) GT3, (b) GT5, and (c) GT7 at 60 GHz.

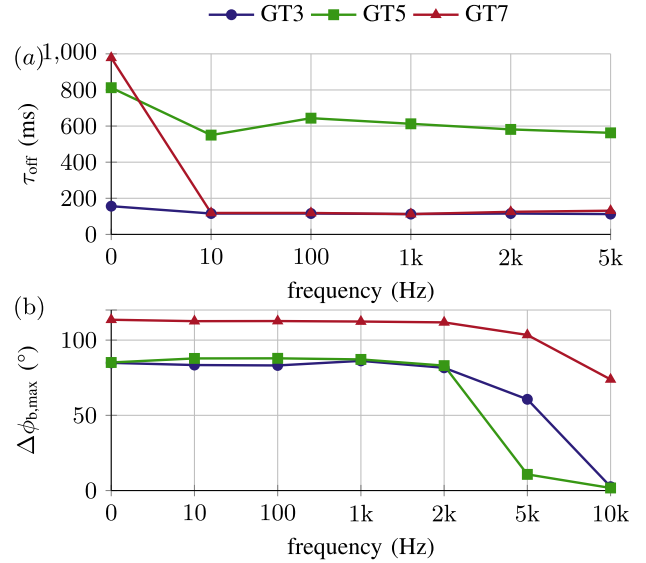


FIGURE 10. Measurement results of the influence of biasing voltage frequency on (a) τ_{off} and (b) $\Delta\phi_{b,max}$ for phase shifters filled with GT3, GT5 and GT7, measured at 60 GHz.

TABLE 3. Performance Comparison of State-of-the-Art Phase Shifters

Technology	f (GHz)	$\Delta\phi_{b,max}$ (°)	IL (dB)	FoM (°/dB)	$\tau_{on/off}$ (s)	$\Delta\phi_{b,max}/\lambda_0$ (°/ λ_0)	Bias Voltage (V)
SiGe [34]	60	28	4	7	/	/	2.4
GaAs [35]	60	360	10.7	33.6	/	/	1
BST [6]	10	342	6.6	52	<0.01	1500	150
MEMS [2]	60	250	3.0	83	/	/	20
LC-MS [16]	17.5	250	4	62.5	>30	63	30
LC-MS [21]	24	350	4.4	80	>200	85	30
LC-DG [13]	95	680	5.2	130	17	70	200
LC-DIL [15]	101	290	3.4	84	5	42	300
LC-VCPW [36]	20	90	1.5	60	0.34	106	40
LC-VMS [22]	20	60	2	30	3	46	40
LC-NaM [29]	60	89	2.9	31	1.3	74	40
LC-NaM This work	56	116	1.7	70	0.12	173	10

demonstrators remain almost unchanged when the bias frequency is below 2 kHz. Above 2 kHz, GT5 shows a severe degradation of tuneability, and becomes almost non-tuneable above 5 kHz, while GT3 and GT7 also suffer a significant decrease in tuneability from 2 kHz to 5 kHz. Near 10 kHz, GT3 becomes non-tuneable, while GT7 still remains at approximately 60% of tuneability. Hence, the optimum bias voltage frequency is approximately 1 kHz. It worth mentioning that each switch-on and switch-off cases has been repeated more than 10 cycles with stable results.

A comparison to state-of-the-art phase shifters is given in Table 3. The FoM of this work is better than that of SiGe and GaAs passive phase shifters. The BST phase shifter shows good compactness, fast response, and comparable FoM but a limited frequency range. MEMS show higher FoMs but with critical application drawbacks introduced in Section I.

The conventional LC-MS reported in [16], [21], [33] results in a phase shifter compactness of $\Delta\phi_{b,max}/\lambda_0$ of $36^\circ/\lambda_0$, $63^\circ/\lambda_0$ and $85^\circ/\lambda_0$, respectively. In this work, it is $173^\circ/\lambda_0$. A miniaturization factor larger than 2 is achieved owing to

NaM technology. The LC layer thicknesses h_{LC} used in [16] and [21] are $100 \mu\text{m}$ and $254 \mu\text{m}$, respectively, while the proposed LC-NaM phase shifter has only $h_{LC} = 4 \mu\text{m}$. [16] and [21] actually reach such comparable FoMs at the expense of an extremely long response time ($> 30 \text{ s}$), which largely limits their application. Response time of [16] and [21] are estimated according to [18], which demonstrates τ_{off} is proportional to h_{LC}^2 . A simulation on conventional LC-MS phase shifter with $h_{LC} = 4 \mu\text{m}$ and $w_{\text{gold}} = 6 \mu\text{m}$ is performed in CST, with $Z_c = 50 \Omega$. However, the FoM peaks at only $10 \text{ }^\circ/\text{dB}$ due to the dramatically high metallic loss, which demonstrates the intrinsic limitation of LC-MS. For LC-NaM, a much wider line width $w_{\text{gold}} = 25 \mu\text{m}$ is maintained to keep 50Ω with $h_{LC} = 4 \mu\text{m}$. Therefore, the SW effect and lower IL together explain the significantly higher FoM than that of LC-MS.

LC varactor-based planar phase shifters are reported in [22]. The authors periodically load a non-tuneable microstrip line with tuneable LC varactors (LC-VMS) connected in series to the line. Although LC is not the substrate for the microstrip line in this topology and h_{LC} of the varactor can be lowered independently of the line's impedance, the limited tuneability of LC-based varactors, complex biasing network and high discontinuity degrade its behaviour. In [36], a CPW is periodically loaded with shunt LC varactors (LC-VCPW), achieving a good FoM, high compactness and fast response. Compared to LC-NaM, their approach has a higher fabrication effort, requires a complex biasing network, limited frequency range due to cut off mechanism and suffers from a distorted wave front when meandered. The previous LC-NaM version [29] utilizing GT3 shows a much lower row measured FoM of $31 \text{ }^\circ/\text{dB}$, a much longer response time of 1.3 s , less compactness and requires much higher bias voltage than both the GT3 and GT7 demonstrators in this work.

The LC-based dielectric waveguide (LC-DG) phase shifter and dielectric image line (LC-DIL) phase shifter in [13] and [15] yield the highest FoM, mainly due to their low loss as a result of fully and partially eliminating the use of metal electrodes, respectively; however, they suffer from a bulky structure and long response time of 17 s and 5 s , respectively. The core region of the DG where the electric field is concentrated should hold the LC, which leads to an LC layer thickness of several hundred μm . This thickness inevitably leads to very long response time. Furthermore, external bias systems are required with complicated electrode design regarding both parasitic strip line mode suppression [37] and proper bias field distribution [15]; their bias voltages are higher than 200 V . For LC-NaM, an additional bias system is not needed since bias can be applied inline through electrodes: In this work for demonstrating purposes, bias is applied directly through the RF probe. In practical applications, highly resistive line is one possible way to conduct bias voltage through which RF signal barely leaks and FoM almost maintains [6], [16], [38]. The low bias voltage gives LC-NaM technology the possibility to be fully integrated into monolithic microwave integrated circuits (MMICs).

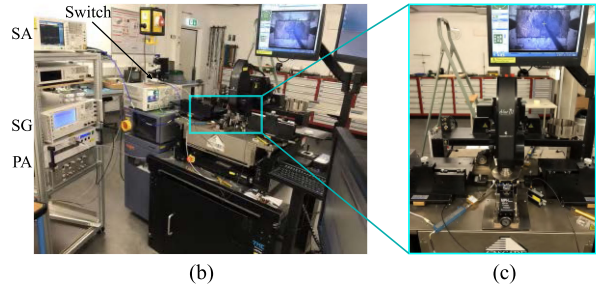
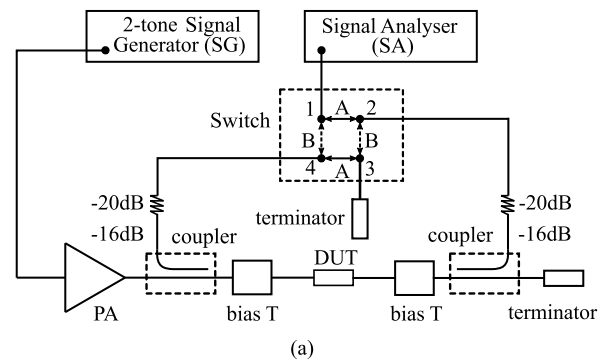


FIGURE 11. Block diagram of the IP3 measurement setup.

IV. LARGE SIGNAL MEASUREMENT

Unwanted higher-order harmonics appear when a large signal propagates through a nonlinear device. The third-order intercept point (IP3) is used to evaluate the device's linearity. Reported LC phase shifters barely consider their linearity, except for [39]. In this work, IP3 measurements are performed in a more accurate manner in which the nonlinearities from the measurement devices are excluded. A combined two-tone signal centred at 6 GHz with multiple frequency separation is generated by Keysight E8267D Vector Signal Generator (SG), and is amplified from -10 dBm up to 35 dBm by a power amplifier (PA) and fed to the phase shifter. The output signals are monitored by Agilent N9020 A MXA Signal Analyser (SA). The measurement setup is shown in Fig. 11. The Agilent 87222 C switch is used to linearize the setup: At each power level, it first switches to path B (Cal path), and pre-distortion by using Keysight Multitone software is performed to remove the nonlinearity of devices in the loop, especially PA. Next, it switches to path A (DUT path), where the detected third-order intermodulation (IMD3) is generated by the DUT only. Measurement results with 1 MHz tone spacing as given in Fig. 12. All three phase shifters have $\text{OIP3} \approx 60 \text{ dBm}$, which indicates a very high linearity of the LC-NaM demonstrators. This result corresponds well with that in [39], the improvement is mainly due to the pre-distortion of the Cal path. A high-power S-parameter measurement is set up as in Fig. 13. Due to PA, only forward transmission S_{21} is measured, and a simple response calibration [40] is performed instead of LRRM method. Results are given in Fig. 14. They indicate that $\Delta\phi_{b,\text{max}}$ remains almost constant until the DUT power reaches 25 dBm and gradually degrades afterwards.

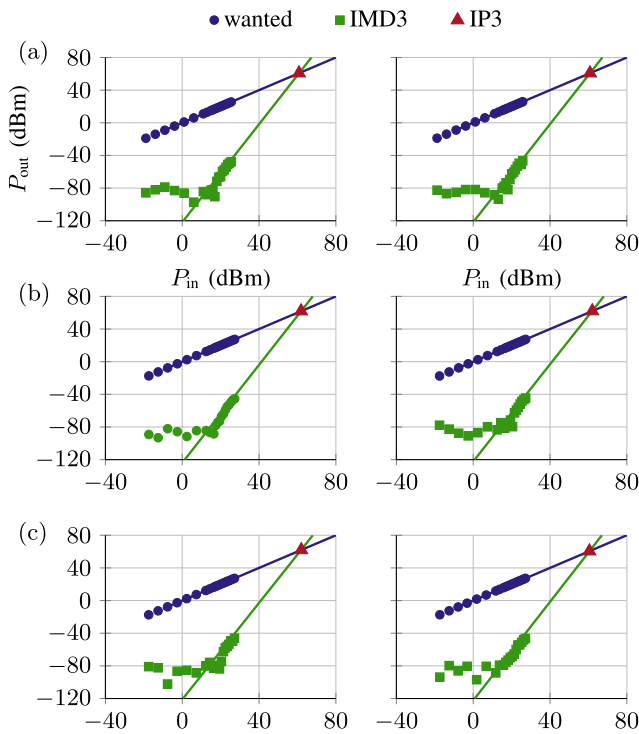


FIGURE 12. IP3 measurements in unbiased case (left column) and fully biased case (right column) for (a) the GT3 demonstrator, (b) the GT5 demonstrator, and (c) the GT7 demonstrator.

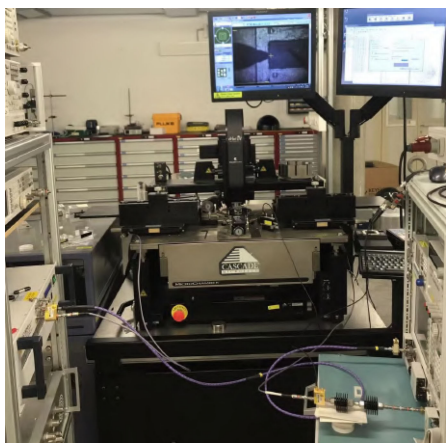
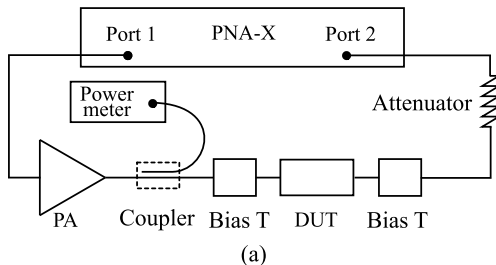


FIGURE 13. Block diagram and photo of the high power S-parameter measurement setup.

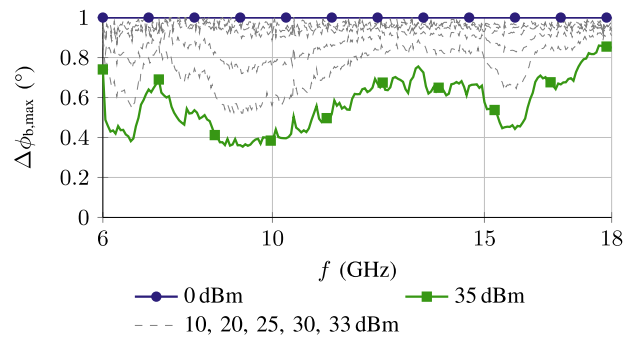


FIGURE 14. Normalized phase shift $\Delta\phi_{b,max}$ measured from 0 dBm to 35 dBm with respect to $\Delta\phi_{b,max}$ at 0 dBm.

V. CONCLUSION AND OUTLOOK

In this paper, an improved highly miniaturized continuously tuneable microstrip phase shifter is presented by combining microwave LC and NaM technology. Compared to the previous version, fabrication process is optimized. Based on this, the performance of the demonstrators are significantly enhanced. Very high FoM, very fast response and compactness are achieved simultaneously for the first time in the realm of LC-based phase shifters. The proposed phase shifters demonstrate a rather simple fabrication procedure with decent reliability and repeatability. The raw measurement results of the GT3, GT5 and GT7 demonstrators all show wide-band matching, with peak FoMs of $41^\circ/\text{dB}$, $48^\circ/\text{dB}$ and $70^\circ/\text{dB}$, respectively. The compactness of the GT7 demonstrator is $173^\circ/\lambda_0$, which is almost double that of the other planar LC phase shifters. This feature makes it rather easy to meander a 360° phase shifter within a $0.5 \lambda_0 \times 0.5 \lambda_0$ area when integrated in antenna arrays.

Based on phase shifters, the frequency of the bias voltage and its effect on the tuneability of the LCs are studied for the first time. 1 kHz square wave is regarded as the optima and LCs start to lose tuneability above 2 kHz. The GT3 and GT7 demonstrators show fast response times of approximately 100 ms. This value is sufficient for most portable applications, such as inter-satellite links from a geostationary relay satellite to a low-earth orbit satellite [41], and for on-the-move applications, such as tracking signals from a satellite by a moving car, ship or airplane [18]. This feature is a great advantage over most LC-based phase shifters. Considering the high FoM, high compactness and fast response, the GT7 demonstrator sets a new benchmark for planar LC phase shifters.

In addition, the large-signal behaviour of the phase shifters is investigated. They show high linearity, with $\text{IP3} \approx 60 \text{ dBm}$ and power handling of 25 dBm. These results indicate the possibility of utilizing LC-based phase shifters in high-power applications. Considering the easy and high-quality through-substrate vias approach on NaM [42], it represents a promising interposer in mmW devices. The combination of NaM and LC should find wide use in miniaturized reconfigurable high data rate communication applications such as phased array antenna systems. Due to the dense distribution of nanowires

inside NaM, the LC-NaM phase shifter can be scaled into the whole microwave frequency range from 300 MHz to 300 GHz.

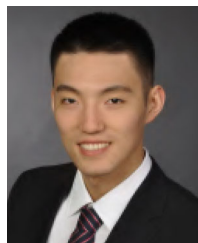
ACKNOWLEDGMENT

The authors thank Merck KGaA, Darmstadt, Germany, for supplying the LC samples; University Sao Paulo, Brazil, for providing the NaM technique; Deutsche Forschungsgemeinschaft (DFG) for funding of this work within project JA921/65-1; and the Open Access Publishing Fund of the Technical University of Darmstadt.

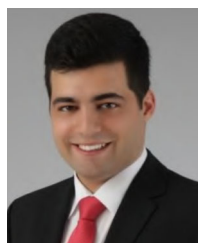
REFERENCES

- [1] A. Stehle *et al.*, "RF-MEMS switch and phase shifter optimized for W-band," in *Proc. 38th Eur. Microw. Conf.*, 2008, pp. 104–107.
- [2] H.-T. Kim *et al.*, "V-band 2-b and 4-b low-loss and low-voltage distributed MEMS digital phase shifter using metal-air-metal capacitors," *IEEE Trans. Microw. Theory Techn.*, vol. 50, no. 12, pp. 2918–2923, Dec. 2002.
- [3] C. won Jung, M.-J. Lee, G. P. Li, and F. De Flaviis, "Reconfigurable scan-beam single-arm spiral antenna integrated with RF-MEMS switches," *IEEE Trans. Antennas Propag.*, vol. 54, no. 2, pp. 455–463, Feb. 2006.
- [4] V. M. Mukhortov, S. I. Masychev, Y. I. Golovko, A. V. Chub, and V. M. Mukhortov, "A phase shifter on a slot line loaded with varactors designed on the basis on nanodimensional films of barium-strontium titanate," *J. Commun. Technol. Electron.*, vol. 52, no. 11, pp. 1300–1304, Nov. 2007. [Online]. Available: <https://doi.org/10.1134/S1064226907110150>
- [5] F. De Flaviis and N. G. Alexopoulos, "Thin ceramic ferroelectric phase shifter for steerable microstrip patch antenna array," in *Proc. 28th Eur. Microw. Conf.*, 1998, vol. 1, pp. 678–683.
- [6] M. Sazegar *et al.*, "Low-cost phased-array antenna using compact tunable phase shifters based on ferroelectric ceramics," *IEEE Trans. Microw. Theory Techn.*, vol. 59, no. 5, pp. 1265–1273, May 2011.
- [7] R. Jakoby, P. Scheele, S. Muller, and C. Weil, "Nonlinear dielectrics for tunable microwave components," in *Proc. 15th Int. Conf. Microw. Radar Wireless Commun.*, 2004, vol. 2, pp. 369–378.
- [8] C. Weickhmann, R. Jakoby, E. Constable, and R. A. Lewis, "Time-domain spectroscopy of novel nematic liquid crystals in the terahertz range," in *Proc. 38th Int. Conf. Infrared Millimeter THz Waves*, 2013, pp. 1–2.
- [9] S. Mueller *et al.*, "Broad-band microwave characterization of liquid crystals using a temperature-controlled coaxial transmission line," *IEEE Trans. Microw. Theory Techn.*, vol. 53, no. 6, pp. 1937–1945, Jun. 2005.
- [10] E. Polat *et al.*, "Characterization of liquid crystals using a temperature-controlled 60 GHz resonator," in *Proc. IEEE MTT-S Int. Microw. Workshop Ser. Adv. Mater. Processes RF THz Appl.*, 2019, pp. 19–21.
- [11] E. Polat *et al.*, "Tunable liquid crystal filter in nonradiative dielectric waveguide technology at 60 GHz," *IEEE Microw. Wireless Compon. Lett.*, vol. 29, no. 1, pp. 44–46, Jan. 2019.
- [12] M. Yazdanpanahi and D. Mirshekar-Syahkal, "Millimeter-wave liquid-crystal-based tunable bandpass filter," in *Proc. IEEE Radio Wireless Symp.*, 2012, pp. 139–142.
- [13] R. Reese *et al.*, "Liquid crystal based dielectric waveguide phase shifters for phased arrays at W-band," *IEEE Access*, vol. 7, pp. 127032–127041, 2019.
- [14] O. H. Karabey, F. Goelden, A. Gaebler, S. Strunck, and R. Jakoby, "Tunable loaded line phase shifters for microwave applications," in *Proc. IEEE MTT-S Int. Microw. Symp.*, 2011, pp. 1–4.
- [15] H. Tesmer, R. Reese, E. Polat, R. Jakoby, and H. Maune, "Dielectric image line liquid crystal phase shifter at W-band," in *Proc. 13th German Microw. Conf.*, 2020, pp. 1–4.
- [16] O. H. Karabey, A. Gaebler, S. Strunck, and R. Jakoby, "A 2-D electronically steered phased-array antenna with 2×2 elements in LC display technology," *IEEE Trans. Microw. Theory Techn.*, vol. 60, no. 5, pp. 1297–1306, May 2012.
- [17] H. Maune, M. Jost, R. Reese, E. Polat, M. Nickel, and R. Jakoby, "Microwave liquid crystal technology," *Crystals*, vol. 8, no. 9, 2018, Art. no. 355.
- [18] R. Jakoby, A. Gaebler, and C. Weickhmann, "Microwave liquid crystal enabling technology for electronically steerable antennas in SATCOM and 5G millimeter-wave systems," *Crystals*, vol. 10, no. 9, 2020, Art. no. 514.
- [19] O. H. Karabey, "Electronic beam steering and polarization agile planar antennas in liquid crystal technology," Ph.D. dissertation, Inst. Microw. Eng. Photon., Technische Universität Darmstadt, Germany, 2013.
- [20] T. Kuki, H. Fujikake, and T. Nomoto, "Microwave variable delay line using dual-frequency switching-mode liquid crystal," *IEEE Trans. Microw. Theory Techn.*, vol. 50, no. 11, pp. 2604–2609, Nov. 2002.
- [21] S. Muller, P. Scheele, C. Weil, M. Wittek, C. Hock, and R. Jakoby, "Tunable passive phase shifter for microwave applications using highly anisotropic liquid crystals," in *IEEE MTT-S Int. Microw. Symp. Dig.*, 2004, vol. 2, pp. 1153–1156.
- [22] W. Hu, O. H. Karabey, A. Gäbler, A. E. Prasetiadi, M. Jost, and R. Jakoby, "Liquid crystal varactor loaded variable phase shifter for integrated, compact, and fast beamsteering antenna systems," in *Proc. 9th Eur. Microw. Integr. Circuit Conf.*, 2014, pp. 660–663.
- [23] K. Rawat and F. M. Ghannouchi, "A design methodology for miniaturized power dividers using periodically loaded slow wave structure with dual-band applications," *IEEE Trans. Microw. Theory Techn.*, vol. 57, no. 12, pp. 3380–3388, Dec. 2009.
- [24] W. Huang, Y. Ren, B. Wang, and W. Luo, "Design of periodic slow-wave transmission line unit with CPW structure," in *Proc. Int. Conf. Microw. Millimeter Wave Technol.*, 2018, pp. 1–3.
- [25] A. Gorur, C. Karpuz, and M. Alkan, "Characteristics of periodically loaded CPW structures," *IEEE Microw. Guided Wave Lett.*, vol. 8, no. 8, pp. 278–280, Aug. 1998.
- [26] A. L. C. Serrano *et al.*, "Slow-wave microstrip line on nanowire-based alumina membrane," in *Proc. IEEE MTT-S Int. Microw. Symp.*, 2014, pp. 1–4.
- [27] A. L. C. Serrano and A. Franc, "Modeling and characterization of slow-wave microstrip lines on metallic-nanowire-filled-membrane substrate," *IEEE Trans. Microw. Theory Techn.*, vol. 62, no. 12, pp. 3249–3254, Dec. 2014.
- [28] A.-L. Franc, F. Podevin, L. Cagnon, P. Ferrari, A. Serrano, and G. Rehder, "Metallic nanowire filled membrane for slow wave microstrip transmission lines," in *Proc. Int. Semicond. Conf. Dresden-Grenoble*, 2012, pp. 191–194.
- [29] M. Jost *et al.*, "Miniaturized liquid crystal slow wave phase shifter based on nanowire filled membranes," *IEEE Microw. Wireless Compon. Lett.*, vol. 28, no. 8, pp. 681–683, Aug. 2018.
- [30] C. Fritzsche and M. Wittek, "Recent developments in liquid crystals for microwave applications," in *Proc. IEEE Int. Symp. Antennas Propag. USNC/URSI Nat. Radio Sci. Meeting*, 2017, pp. 1217–1218.
- [31] G. Zheng, J. Papapolymerou, and M. M. Tentzeris, "Wideband coplanar waveguide RF probe pad to microstrip transitions without via holes," *IEEE Microw. Wireless Compon. Lett.*, vol. 13, no. 12, pp. 544–546, Dec. 2003.
- [32] L. Zhu and K. L. Melde, "On-wafer measurement of microstrip-based circuits with a broadband vialess transition," *IEEE Trans. Adv. Packag.*, vol. 29, no. 3, pp. 654–659, Aug. 2006.
- [33] S. Bulja and D. Mirshekar-Syahkal, "Meander line millimetre-wave liquid crystal based phase shifter," *Electron. Lett.*, vol. 46, no. 11, pp. 769–771, 2010.
- [34] A. Bautista, A. Franc, and P. Ferrari, "Accurate parametric electrical model for slow-wave CPW and application to circuits design," *IEEE Trans. Microw. Theory Techn.*, vol. 63, no. 12, pp. 4225–4235, Dec. 2015.
- [35] K. Han, H. Cui, X. Sun, and J. Zhang, "The design of a 60 GHz low loss hybrid phase shifter with 360 degree phase shift," in *Proc. 14th Int. Symp. Commun. Inf. Technol.*, 2014, pp. 551–554.
- [36] F. Goelden, A. Gaebler, M. Goebel, A. Manabe, S. Mueller, and R. Jakoby, "Tunable liquid crystal phase shifter for microwave frequencies," *Electron. Lett.*, vol. 45, no. 13, pp. 686–687, 2009.
- [37] R. Reese *et al.*, "A millimeter-wave beam-steering lens antenna with reconfigurable aperture using liquid crystal," *IEEE Trans. Antennas Propag.*, vol. 67, no. 8, pp. 5313–5324, Aug. 2019.

- [38] D. Wang, E. Polat, H. Tesmer, R. Jakoby, and H. Maune, "A compact and fast 1×4 continuously steerable endfire phased-array antenna based on liquid crystal," *IEEE Antennas Wireless Propag. Lett.*, vol. 20, no. 10, pp. 1859–1862, Oct. 2021.
- [39] F. Goelden, S. Mueller, P. Scheele, M. Wittek, and R. Jakoby, "IP3 measurements of liquid crystals at microwave frequencies," in *Proc. Eur. Microw. Conf.*, 2006, pp. 971–974.
- [40] W. Zheng, C. E. Smith, and L. Wang, "Response calibration for automated network analyzer systems," in *Proc. 25th Southeastern Symp. Syst. Theory*, 1993, pp. 29–33.
- [41] M. Tebbe, A. Hoehn, N. Nathrath, and C. Weickmann, "Simulation of an electronically steerable horn antenna array with liquid crystal phase shifters," in *Proc. IEEE Aerosp. Conf.*, 2016, pp. 1–15.
- [42] J. M. Pinheiro *et al.*, "110-GHz through-substrate-via transition based on copper nanowires in alumina membrane," *IEEE Trans. Microw. Theory Techn.*, vol. 66, no. 2, pp. 784–790, Feb. 2018.



DONGWEI WANG was born in Taiyuan, Shanxi, China, in 1991. He received the B.Eng. degree from Zhejiang University, Hangzhou, Zhejiang, China, and the M.Sc. degree from Karlsruhe Institut für Technologie, Karlsruhe, Germany. He is currently working toward the Ph.D. degree with the Institute of Microwave Engineering and Photonics, Technische Universität Darmstadt, Darmstadt, Germany. His current research focuses on liquid crystal-based tunable planar devices with Slow-wave effect.



ERSIN POLAT (Student Member, IEEE) was born in Alzenau, Germany, in 1991. He received the B.Sc. and M.Sc. degrees from Technische Universität Darmstadt, Darmstadt, Germany, in 2014 and 2017, respectively, where he is currently working toward the Ph.D. degree with the Microwave Engineering Group. His current research interests include tunable microwave filters and material characterization.



CHRISTIAN SCHUSTER (Student Member, IEEE) was born in Wiesbaden, Germany, in 1988. He received the B.Sc. and M.Sc. degrees from Technische Universität Darmstadt, Darmstadt, Germany, in 2012 and 2015, respectively, where he is currently working toward the Ph.D. degree with the Microwave Engineering Group. His research interests include tunable microwave filters and reconfigurable RF transceiver systems.



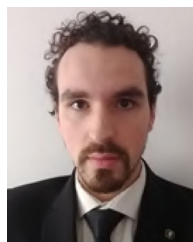
HENNING TESMER (Student Member, IEEE) was born in Kassel, Germany, in 1992. He received the B.Sc. and M.Sc. degrees from Technische Universität Darmstadt, Darmstadt, Germany, in 2015 and 2018, respectively, where he is currently working toward the Ph.D. degree with the Institute of Microwave Engineering and Photonics. His current research interests include liquid crystal-based tunable dielectric waveguides and components for millimeter-wave applications.



GUSTAVO P. REHDER (Member, IEEE) was born in São Paulo, Brazil, in 1979. He received the B.S. degree in electrical engineering from Arkansas State University, Jonesboro, AK, USA, in 2003, and the M.S. and Ph.D. degrees in electrical engineering from the University of São Paulo, São Paulo, Brazil, in 2005 and 2008, respectively. From 2009 to 2011, he was a Postdoctorate with TIMA Laboratory, Grenoble, France, and then the Institut de Microélectronique Electromagnétisme et Photonique and Laboratoire d'Hyperfréquences et de Caractérisation, Grenoble, France, where he initiated the development of microelectromechanical systems (MEMS)-based tunable phase shifters for millimeter-wave applications. He is currently a Researcher and Professor with the Laboratory of Microelectronics, Polytechnic School, University of São Paulo. His research interests include modeling, fabrication, and test of RF MEMS devices.



ARIANA L. C. SERRANO (Member, IEEE) was born in São Paulo, Brazil, in 1976. She received the Electrical Engineering and M.Sc. degrees from the Polytechnic School, University of São Paulo, São Paulo, Brazil, in 1999 and 2007, respectively, and the Ph.D. degree from the University of São Paulo and the Grenoble Institute of Technology, Grenoble, France. In 2011, she joined the Institut de Microélectronique Electromagnétisme et Photonique and Laboratoire d'Hyperfréquences et de Caractérisation, Grenoble, France, as a Postdoctorate, where she initiated the development of slow-wave devices on millimeter-wave frequencies. She was with Nortel Networks, where she was involved in telecommunications systems. From 2003 to 2008, she was with Thales/Omnisys, where she was involved in the development of RF hardware, especially radars and satellites. She is currently an Associate Professor with the University of São Paulo. She holds two patents. Her current research interests include planar microwave filters, reconfigurable and tunable circuits and millimeter-wave passive devices—modeling and characterization, and also slow-wave devices.



LEONARDO G. GOMES (Graduate Student Member, IEEE) received the bachelor's degree in electrical engineering and the Master of Science degree from the University of São Paulo, São Paulo, Brazil, in 2015 and 2017, respectively. He is currently working toward the Ph.D. degree with the University of São Paulo and Communauté Université Grenoble-Alpes. He worked on mm-waves circuits and devices and microelectronics fabrication on novel interposer technologies at his master thesis. He is currently working on the development of a 60 GHz phased array on a novel interposer technology and on a mm-wave VCO on BiCMOS technology for his Ph.D. thesis. His research interests include the design of passive, mm-wave devices and circuits, and the design of active circuits on mm-waves.



PHILIPPE FERRARI (Senior Member, IEEE) received the M.Sc. degree in electrical engineering and the Ph.D. degree from the Institut National Polytechnique de Grenoble, Grenoble, France, in 1989 and 1992, respectively. In 1992, he joined the Laboratory of Microwaves and Characterization, University of Savoy, Chambéry, France, as an Assistant Professor of electrical engineering, and was involved in the development of RF characterization techniques. From 1998 to 2004, he was the Head of laboratory project on nonlinear transmission lines and tunable devices. Since 2004, he has been a Professor with Grenoble-Alpes University, France, and he has been continues his research with the Institut de Microélectronique Electromagnétisme et Photonique and Laboratoire d'Hyperfréquences et de Caractérisation, since 2007. He is currently the Head of the RF and Millimeter-Wave Group (RFM). His main research interests include tunable and miniaturized devices, such as filters, phase shifters, matching networks and power dividers, and new circuits based on slow-wave transmission lines, at millimeter-wave frequencies, in CMOS and BiCMOS technologies.



HOLGER MAUNE (Senior Membr, IEEE) was born in Cologne, Germany, in 1981. He received the Dipl.-Ing., Dr.-Ing., and the *venia legend* degrees in communications engineering from the Technische Universität Darmstadt, Darmstadt, Germany, in 2006, 2011, and 2020, respectively. Since 2021, he has been Full Professor of electrical engineering and holds the Chair of Microwave and Communication Engineering with the University of Magdeburg, Magdeburg, Germany. His research interests include reconfigurable smart radio

frequency (RF) systems based on electronically tunable microwave components such as phase shifters, adaptive matching networks, tunable filters, duplexer, and multiband antennas. Their integration into system components such as adaptively matched power amplifiers, reconfigurable RF frontends or fully integrated electronically beam-steering transceiver antenna arrays is in the focus of the work. The tunable microwave components are based on novel approaches and innovative functional materials and technologies such as ferroelectric (BST) thin- and thick films and microwave liquid crystals (LC). Beyond novel concepts and design, a main interest is on modeling and precise high-frequency characterization, such as by means of scattering parameter measurements in dependence of frequency, temperature and static field strengths. Moreover, dedicated functional tests such as intermodulation and harmonic distortion are of major interest.



ROLF JAKOBY (Member, IEEE) was born in Kinheim, Germany, in 1958. He received the Dipl.-Ing. and Dr.-Ing. degrees in electrical engineering from the University of Siegen, Siegen, Germany, in 1985 and 1990, respectively. In 1991, he joined the Research Center of Deutsche Telekom, Darmstadt, Germany. Since 1997, he has been a Full Professor with Technische Universität Darmstadt, Darmstadt, Germany. He is currently a Co-Founder of ALCAN Systems GmbH. He has authored more than 320 publications and holds

more than 20 patents. His current research interests include chipless RFID sensor tags, biomedical sensors and applicators, and tunable passive microwave/millimeter wave devices and beam-steering antennas, using primarily ferroelectric and liquid crystal technologies.

Dr. Jakoby is a member of VDE/ITG and IEEE/MTT/AP societies. He was the recipient of the Award from CCI Siegen for his excellent Ph.D. thesis, in 1992, and the ITG-Prize for an excellent publication in *IEEE TRANSACTIONS ON ANTENNAS AND PROPAGATION*, in 1997. His group was the recipient of the 21 awards and prizes for best papers and doctoral dissertations. He was the Chairman of the EuMC, in 2007, and GeMiC, in 2011, and a Treasurer of the EuMW, in 2013 and 2017. He is the Editor-in-Chief of *FREQUENZ* (DeGruyter).